Machine Vision and Applications (2004) 15: 194–203
Digital Object Identifier (DOI) 10.1007/s00138-004-0149-2

Machine Vision and Applications

Feature extraction of finger-vein patterns based on repeated line tracking and its application to personal identification

Naoto Miura, Akio Nagasaka, Takafumi Miyatake

HITACHI, Ltd. 1-280 Higashi-koigakubo, Kokubunji-shi, Tokyo, 185-8601, Japan (e-mail: {n-miura,akio-n,miyatake}@crl.hitachi.co.jp)

Received: 27 October 2003 / Accepted: 25 February 2004
Published online: 21 July 2004 –

Abstract. We propose a method of personal identification based on finger-vein patterns. An image of a finger captured under infrared light contains not only the vein pattern but also irregular shading produced by the various thicknesses of the finger bones and muscles. The proposed method extracts the finger-vein pattern from the unclear image by using line tracking that starts from various positions. Experimental results show that it achieves robust pattern extraction, and the equal error rate was 0.145% in personal identification.

Keywords: Personal identification – Biometrics – Finger vein – Feature extraction – Line tracking

1 Introduction

Personal identification technology is applied to a wide range of systems including area-access control, PC login, and e-commerce. Biometrics is the statistical measurement of human physiological or behavioral traits. Biometric techniques for personal identification have been attracting attention recently because conventional means such as keys, passwords, and PIN numbers have problems in terms of theft, loss, and reliance on the user's memory.

In the area of biometric identification, security and convenience of the system are important [1]. In particular, the systems require high accuracy and fast response times. Biometric methods include those based on the pattern of fingerprints [9–11], facial features [18], the iris [14], the voice [15], the hand geometry [13], or the veins on the back of the hand [12]. However, these methods do not necessarily ensure confidentiality because the features used in the methods are exposed outside the human body. These methods can therefore be susceptible to forgery.

To solve this problem, we proposed a biometric system using patterns of veins within a finger, that is, patterns inside the human body [2,3]. In this system, an infrared light is transmitted from the backside of the hand. A finger is placed between the infrared light source and camera. As hemoglobin in the blood absorbs the infrared light, the pattern of veins in the palm side of the hand is captured as a pattern of shadows.

The captured images contain not only vein patterns but also irregular shading and noise. The shading is produced by the varying thickness of finger bones and muscles. Therefore, regions in which the veins are and are not sharply visible exist in a single image.

To develop highly accurate personal identification systems, finger-vein patterns should be extracted precisely from the captured images, and the process must be executed speedily in order to satisfy requirements for user convenience.

Conventional methods for extracting line-shaped features from images include the matched-filter method [4], mathematical morphology [5], connection of emphasized edge lines [6], and ridge line following for minutiae detection in grayscale fingerprint images [11]. The matched-filter and morphological methods can execute fast feature extraction because all that's required is to filter the image. However, this can also emphasize irregular shading, which presents an obstacle to personal identification since this obscures parts of the pattern of veins. Moreover, dots of noise are also emphasized because continuity is not considered.

When the connection of emphasized edge lines is used to extract a finger-vein pattern, line extraction can be executed if one takes into account continuity. However, the differential operation and optimization of the line connections carry immense computational costs. It may take ten or more minutes to process an image. Therefore, this method is not suitable when real-time processing is required.

The minutiae detection algorithm [11] is based on ridge line following. The ridge line following, which is executed by checking the local darkest position in the cross-sectional profiles, works well if the ridge appears clearly. However, finger-vein images are not clear enough for this method to be used.

In this paper, we propose a method that solves the problems described above. The method is based on line tracking, which starts at various positions. Local dark lines are identified, and line tracking is executed by moving along the lines, pixel by pixel. When a dark line is not detectable, a new tracking operation starts at another position. All the dark lines in the image can be tracked by repeatedly executing such local line-tracking operations. Finally, the loci of the lines overlap and the pattern of finger veins is obtained statistically. As the parts of the dark lines are tracked again and again in the repeated

operations, they are increasingly emphasized. Although noise may also be tracked, noise is emphasized to a smaller degree than the dark lines. This makes line extraction robust. Furthermore, reduction of the number of tracking operations and the spatial reduction of the pattern can reduce computational costs.

2 Personal identification using finger-vein patterns

2.1 Procedure for personal identification

The procedure for personal identification by using patterns of veins in a finger is shown in Fig. 1. The details are described below.

Step 1 : Acquisition of an infrared image of the finger

A special imaging device is used to obtain the infrared image of the finger. An infrared light irradiates the backside of the hand and the light passes through the finger. A camera located in the palm side of the hand captures this light. The intensity of light from the LED is adjusted according to the brightness of the image. Figure 2a shows a prototype imaging device. It is 7 cm (wide) $\times$ 6 cm (long) $\times$ 4 cm (high) and has a 1/3-inch CCD camera. The device is constructed of inexpensive parts.

As hemoglobin in the blood absorbs the infrared light, the pattern of veins in the palm side of the finger are captured as shadows. Moreover, the transmittance of infrared light varies with the thickness of the finger. Since this varies from place to place, the infrared image contains irregular shading. In Fig. 2, b and c are examples of the captured images.

Each image is grayscale, 240×180 pixels in size, with 8 bits per pixel. The length of the finger is in the horizontal direction, and the fingertip is on the right side of the image.

Step 2 : Normalization of the image

The location and angle of the finger in the image require some form of normalization, since these qualities will vary each time. Two-dimensional normalization is done using the outline of the finger on the assumption that the three-dimensional location and angle of the finger are constant.

Step 3 : Extraction of finger-vein patterns

The finger-vein pattern is extracted from the normalized infrared image of the finger.

Step 4 : Matching

The correlations between the input pattern and all the registered patterns are calculated.

Step 5 : Output of the result of identification

When the pattern is identified as a registered pattern, the required action, such as unlocking a door or logging onto a PC, is performed.

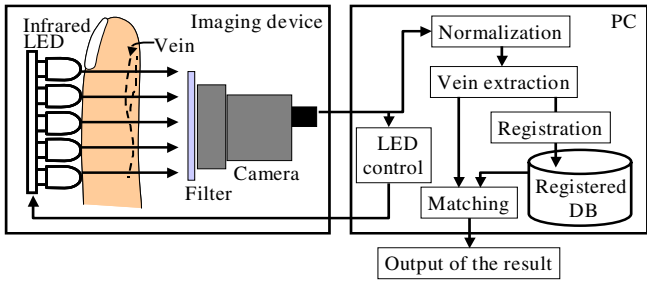

Fig. 1. Principle of personal identification using finger-vein patterns

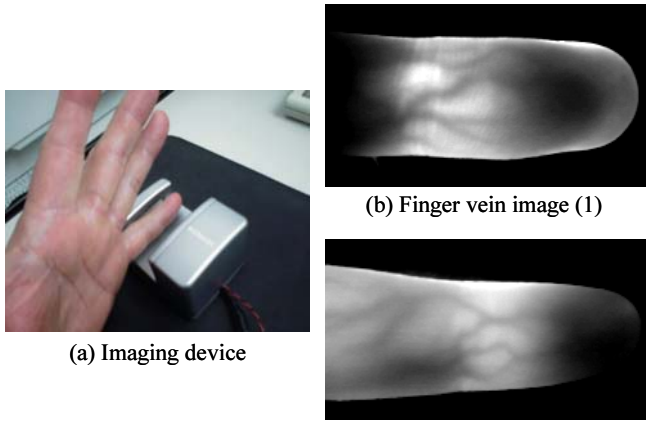

(a) Imaging device

(b) Finger vein image (1)

(c) Finger vein image (2)

Fig. 2. Prototype of finger-vein imaging device (**a**) and examples of infrared images of a finger (**b**, **c**)

2.2 Technical issues

The technical issues for a personal identification system based on finger-vein patterns are (i) robust extraction of the patterns of finger veins despite the presence of irregular shading and noise and (ii) fast identification.

To execute personal identification to a high degree of accuracy, only the pattern of veins should be extracted from the infrared image. However, the image also contains irregular shading and noise (Figs. 2b and c). A practical personal identification system thus requires robustness against these factors.

In order to satisfy the user convenience of the personal identification system, the response time should be no more than 1 s in general. Therefore, we aim to achieve a response time within this range.

3 Extracting and matching the finger-vein patterns

3.1 Keeping extraction robust against irregular shading and noise

For robust extraction of the finger-vein patterns from the nonuniform images, our methods include the repeated tracking of dark lines in the images. Extraction of the patterns is based on the number of times the tracking lines pass through the points.

3.1.1 Repeated trials of dark-line tracking

A cross-sectional profile of a vein appears as a valley, as shown in Fig. 3. The depth of the valley varies with the shading in the image. However, the valley remains detectable. Therefore, the profiles give us a robust method of finger-vein detection.

The line-tracking operation starts at any pixel in the captured image. The current pixel position is called the "current tracking point", and it is moved pixel by pixel along the dark line. The depth of the cross-sectional profile is checked around the current tracking point. Figure 4 shows an example of the spatial relationship between the current tracking point (x_c, y_c) and the cross-sectional profile. Pixel p is a neighbor of the current tracking point in the upper-right direction. Cross-sectional profile s-p-t looks like a valley. Therefore, the current tracking point is on a dark line. The direction of this dark line can be detected by checking the depth of the valley with varying θ_i. This gives us the θ_i at which the valley is deepest. After that, the current tracking point moves to the pixel closest to this direction, pixel p. If the valley is not detectable in any direction θ_i, the current tracking point is not on a dark line and a fresh tracking operation starts at another position.

For smooth line tracking, an attribute that restricts increases in the global curvature of the locus is added to the tracking point. This attribute is called "the moving-direction attribute". In concrete terms, this restricts selection from among the eight neighboring pixels of the next tracking-point position.

If only a single line-tracking operation is conducted, only a part of veins within the image will be tracked. To solve this problem, vein-tracking sequences are started at various positions that are determined so that the line-tracking trials are conducted evenly across the image.

The current tracking point may track a region of noise by chance. Statistically, however, the dark lines are increasingly tracked more often with repeated operations. This makes for the robust extraction of patterns of finger veins.

The number of times that each pixel has become the current tracking point is recorded in a matrix named the "locus space". The size of the locus space is the same as the number of pixels in the captured images. The total number of trials on which each pixel has become the current tracking point is recorded in the corresponding matrix element. Therefore, an element of the locus space that is more frequently tracked has a higher value.

3.1.2 Extraction of the finger-vein patterns

The positions in the locus space where high values are stored are those tracked frequently in the line-tracking procedure. That is, the positions with high values in the locus space have high probabilities of being the positions of veins.

Therefore, the paths of finger veins are obtained as chains of high-value positions in the locus space.

3.2 Reducing computational costs

3.2.1 Eliminating unnecessary tracking operations

In the procedure of repeated line tracking, when tracking begins from tracking points near each other, tracking follows similar paths. Therefore, line tracking from all pixels in the finger region is not required. Eliminating some start points for line tracking reduces the computational costs while retaining accuracy in extraction. In this study, the starting point for each line-tracking operation is determined by using the Monte Carlo method [7].

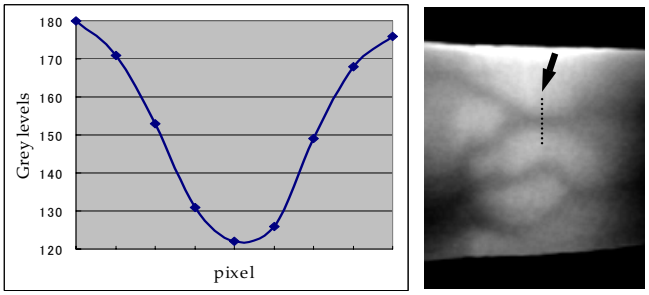

a b

Fig. 3a,b. Cross-sectional brightness profile of a vein. **a** Cross-sectional profile. **b** Position of cross section

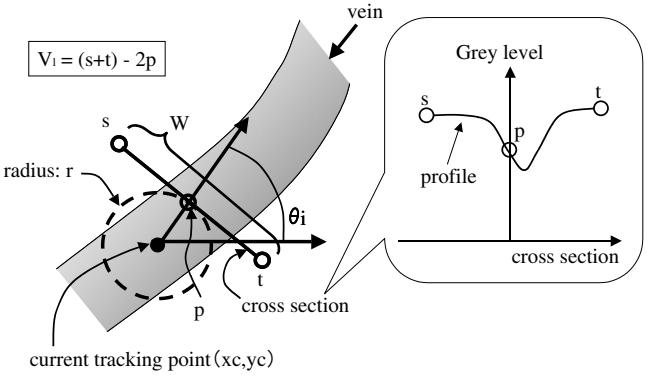

Fig. 4. Dark-line detection

3.2.2 Reducing the size of the pattern

The smaller the template, the faster the computation; that is, reducing the size of the locus space leads to faster computation. Since the pattern of veins has a sparse structure in general, the information required for personal identification is retained.

3.3 Algorithms

3.3.1 Feature extraction

The method of feature extraction is described in this section. $F(x, y)$ is the intensity of the pixel (x, y), (x_c, y_c) is the position of the current tracking point of line tracking in the image, R_f is the set of pixels within the finger's outline, and T_r is the locus space. Suppose the pixel in the lower left in the image to be $(0, 0)$, the positive direction of the x-axis to be rightward in the image, the positive direction of the y-axis to be upward within the image, and $T_r(x, y)$ to be initialized to 0.

Step 1: Determination of the start point for line tracking and the moving-direction attribute

Step 2 : Detection of the direction of the dark line and movement of the tracking point
Step 3 : Updating the number of times points in the locus space have been tracked
Step 4 : Repeated execution of step 1 to step 3 (N times)
Step 5 : Acquisition of the finger-vein pattern from the locus space

The details of each step are described below.

Step 1 : Determination of the start point for line tracking and the moving-direction attribute.

The start point for line tracking is (x_s, y_s), a pair of uniform random numbers selected from R_f. That is, the initial value of the current tracking point (x_c, y_c) is (x_s, y_s). After that, the moving-direction attribute D_{lr}, D_{ud} is determined. D_{lr}, D_{ud} are the parameters that prevent the tracking point from following a path with excessive curvature. D_{lr} and D_{ud} are independently determined as follows:

$$D_{lr} = \begin{cases} (1,0) & (\text{if } R_{nd}(2) < 1). \\ (-1,0) & (\text{otherwise}); \end{cases} \quad (1)$$

$$D_{ud} = \begin{cases} (0,1) & (\text{if } R_{nd}(2) < 1). \\ (0,-1) & (\text{otherwise}), \end{cases} \quad (2)$$

where $R_{nd}(n)$ is a uniform random number between 0 and n.

Step 2 : Detection of the dark-line direction and movement of the tracking point

This step is composed of several substeps.

Step 2-1 : Initialization of the locus-position table T_c
Step 2-2 : Determination of the set of pixels N_c to which the current tracking point can move
Step 2-3 : Detection of the dark-line direction near the current tracking point
Step 2-4 : Registration of the locus in the locus-position table T_c and moving of the tracking point
Step 2-5 : Repeated execution of steps 2-2 to 2-4

Details of these steps are described below.

Step 2-1 : Initialization of the locus-position table T_c

The positions that the tracking point moves to are stored in the locus-position table, T_c. The table is initialized in this step.

Step 2-2 : Determination of the set of pixels N_c to which the current tracking point can move

A pixel to which the current tracking point (x_c, y_c) moves must be within the finger region, have not been a previous (x_c, y_c) within the current round of tracking, and be one of the neighboring pixels of (x_c, y_c).

Therefore, N_c is determined as follows:

$$N_c = \overline{T_c} \cap R_f \cap N_r(x_c, y_c), \quad (3)$$

where $N_r(x_c, y_c)$ is the set of neighboring pixels of (x_c, y_c), selected as follows:

$$N_r(x_c, y_c) = \quad (4)$$
$$\begin{cases} N_3(\boldsymbol{D}_{lr})(x_c, y_c) & (\text{if } R_{nd}(100) < p_{lr}); \\ N_3(\boldsymbol{D}_{ud})(x_c, y_c) & (\text{if } p_{lr}{+}1 \le R_{nd}(100) < p_{lr}{+}p_{ud}); \\ N_8(x_c, y_c) & (\text{if } p_{lr}{+}p_{ud}{+}1 \le R_{nd}(100)), \end{cases}$$

where $N_8(x, y)$ is the set of eight neighboring pixels of a pixel (x_c, y_c) and $N_3(\boldsymbol{D})(x, y)$ is the set of three neighboring pixels of (x_c, y_c) whose direction is determined by the moving-direction attribute $\boldsymbol{D}$ (defined as (D_x, D_y)).
$N_3(\boldsymbol{D})(x, y)$ can be described as follows:

$$\begin{aligned} N_3(\boldsymbol{D})(x, y) = \{&(D_x{+}x,\ D_y{+}y), \\ &(D_x{-}D_y{+}x,\ D_y{-}D_x{+}y), \\ &(D_x{+}D_y{+}x,\ D_y{+}D_x{+}y)\}. \end{aligned} \quad (5)$$

Parameters p_{lr} and p_{ud} in Eq. 4 are the probability of selecting the three neighboring pixels in the horizontal or vertical direction, respectively, as $N_r(s_c, y_c)$. The veins in a finger tend to run in the direction of the finger's length. Therefore, if we increase the probability that $N_3(\boldsymbol{D}_{lr})(x_c, y_c)$ is selected as $N_r(x_c, y_c)$, we obtain a faithful representation of the pattern of finger veins. In preliminary experiments, excellent results are produced when $p_{lr} = 50$ and $p_{ud} = 25$.

Step 2-3 : Detection of the dark-line direction near the current tracking point

To determine the pixel to which the current tracking point (x_c, y_c) should move, the following equation, referred to as the line-evaluation function, is calculated. This reflects the depth of the valleys in the cross-sectional profiles around the current tracking point (Fig. 4):

$$\begin{aligned} V_l = \max_{(x_i, y_i) \in N_c} \Bigg\{ & \\ & F(x_c{+}r\cos\theta_i{-}\frac{W}{2}\sin\theta_i,\ y_c{+}r\sin\theta_i{+}\frac{W}{2}\cos\theta_i) \\ & {+}F(x_c{+}r\cos\theta_i{+}\frac{W}{2}\sin\theta_i,\ y_c{+}r\sin\theta_i{-}\frac{W}{2}\cos\theta_i) \\ & {-}2F(x_c{+}r\cos\theta_i,\ y_c{+}r\sin\theta_i)\Bigg\}, \end{aligned} \quad (6)$$

where W is the width of the profiles, r is the distance between (x_c, y_c) and the cross section, and θ_i is the angle between the line segments $(x_c, y_c) - (x_c + 1, y_c)$ and $(x_c, y_c) - (x_i, y_i)$. In this paper, in consideration of a thickness of the veins that are visible in the captured images, these parameters are set at $W = 11$ and $r = 1$.

Step 2-4 : Registration of the locus in the locus-position table T_c and moving of the tracking point

The current tracking point (x_c, y_c) is added to the locus-position table T_c. After that, if V_l is positive, (x_c, y_c) is then updated to (x_i, y_i) where V_l is maximum.

Step 2-5 : Repeated execution of steps 2-2 to 2-4

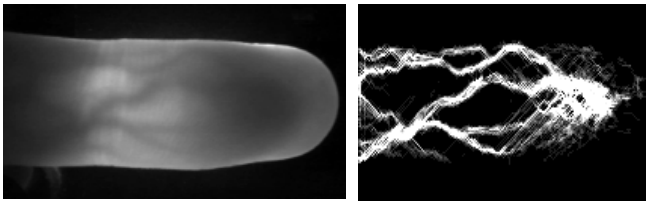

a **b**

Fig. 5a,b. Effectiveness of finger-vein-pattern extraction. **a** Infrared image. **b** Value distribution in the locus space

If V_l is positive, go to step 2-2; if V_l is negative or zero, leave step 2 and go to step 3, since (x_c, y_c) is not on the dark line.

Step 3 : Updating the number of times points in the locus space have been tracked

Values of elements in the locus space $T_r(x, y)$ are incremented $\forall(x, y) \in T_c$.

Step 4 : Repeated execution of steps 1 to 3 (N times)

Steps 1 to 3 are thus executed N times. If the number of repetitions N is too small, insufficient feature extraction is performed. If, on the other hand, N is too big, computational costs are needlessly increased. Through an experiment, we determined that $N = 3000$ is the lower limit for sufficient feature extraction (Sect. 4.1).

Step 5 : Acquisition of the pattern of veins from the locus space

The total number of times the pixel (x, y) has been the current tracking point in the repetitive line tracking operation is stored in the locus space, $T_r(x, y)$. Therefore, the finger-vein pattern is obtained as chains of high values of $T_r(x, y)$. Figure 5 shows a result of finger-vein extraction. Figure 5a is the infrared image from which Fig. 5b is produced as the distribution of values in $T_r(x, y)$. The higher values are shown as brighter pixels.

3.3.2 Matching

In the matching process, the pattern is converted into matching data, and these data are compared with recorded data.

Two methods are commonly used for matching line-shaped patterns: structural matching [17] and template matching [8,16].

Structural matching requires additional extraction of feature points such as line endings and bifurcations. Since a finger-vein pattern has few of these points, template matching based on comparison of pixel values is more appropriate for finger-vein pattern matching.

The conventional template-matching technique is not robust against pattern distortion [16]. To solve this problem, the "ambiguous regions" around the veins are identified, and the slight misalignments between vein patterns in these regions are ignored. Robust template-matching is thereby achieved.

The matching process is as follows.

Step 1 : Labeling of the locus space
Step 2 : Spatial reduction and relabeling of the locus space
Step 3 : Matching of data

The details of these steps are as follows:

Step 1 : Labeling of the locus space

The locus space is binarized by using a threshold. Pixels with values smaller than the threshold are labeled as parts of the background, and those with values greater than or equal to the threshold are labeled as parts of the vein region. In this study, the threshold is determined such that the dispersion between the groups of values in the locus space is maximized, assuming that the histogram of values in the locus space is diphasic in form. We define the values of pixels labeled as parts of the background as 0 and of pixels labeled as parts of the vein regions as 255.

Step 2 : Spatial reduction and relabeling of the locus space

To create matching data, spatial reduction and relabeling of the locus space are performed. In order to retain veins as small as about 3 pixels in the image, the locus space is reduced to one third of its original size in both dimensions. This reduction is accomplished by taking the averages of all nonoverlapping 3×3 pixels.

The binarized (0 or 255) image of the locus space is turned into a smaller grayscale image. When this new locus space is rebinarized by simply setting the threshold to 128, aliasing appears around the borders between the background and the veins. Therefore, the thin lines that have the same shape tend to be misaligned with each other.

To solve this problem, those pixels that have intermediate-range value are treated as ambiguous regions that are not necessarily part of either the background or finger-vein region. In this study, pixel values in the range 0 to 85 are converted to 0, which represents the background region, pixel values in the range 86 to 170 are converted to 128, which represents the ambiguous regions, and pixel values in the range 171 to 255 are converted to 255, which represents the veins.

Step 3 : Matching of data

In this step, a mismatch ratio R_m is calculated to examine whether or not two sets of data have a correlation with each other. The ratio R_m is defined as the difference between two sets of data to be matched. $R(x, y)$ and $I(x, y)$ are the values at position (x, y) of the registered and input matching data, w and h are the width and height of both sets of data, c_w and c_h are the distances in which motion in the vertical and horizontal directions, respectively, is required to adjust the displacement between the two sets of data, and the template data are defined as the rectangular region within $R(x, y)$ whose upper-left position is $R(c_w, c_h)$ and lower-right position is $R(w - c_w, h - c_h)$.

The value of mismatch $N_m(s, t)$, which is the difference between the registered and input data at the positions where $R(c_w, c_h)$ overlaps with $I(s, t)$, is defined as follows:

$$N_m(s,t) = \sum_{y=0}^{h-2c_h-1} \sum_{x=0}^{w-2c_w-1} \Big\{ \phi(I(s+x, t+y), R(c_w+x, c_h+y)) \Big\}, \quad (7)$$

where $w = 66$ and $h = 44$ in consideration of the finger size in the captured image, c_w and c_h are set at $c_w = 8$ and $c_h = 7$ in order to adjust the finger position in the captured image by up to about 1 cm, and ϕ in Eq. 7 is a parameter that indicates whether a pixel labeled as part of the background region and a pixel labeled as part of a vein region overlapped with each other. When P_1 is defined as the pixel value of one pixel and P_2 is defined as the pixel value of the other pixel, ϕ can be described as follows:

$$\phi(P_1, P_2) = \begin{cases} 1 & \text{if } |P_1 - P_2| = 255 \\ 0 & \text{otherwise.} \end{cases} \quad (8)$$

The minimum value of mismatch N_m, which is the smallest $N_m(s,t)$ calculated under the condition that the template overlaps with the input matching data $I(x,y)$ at all positions, can be defined as follows:

$$N_m = \min_{0 \le s < 2c_w, 0 \le t < 2c_h} N_m(s,t). \quad (9)$$

Using the definitions given above, the mismatch ratio R_m is defined as follows:

$$R_m = N_m / \left\{ \sum_{j=t_o}^{t_o+h-2c_h-1} \sum_{i=s_o}^{s_o+w-2c_w-1} \phi(I(i,j),0) + \sum_{j=c_h}^{h-c_h-1} \sum_{i=c_w}^{w-c_w-1} \phi(0, R(i,j)) \right\}, \quad (10)$$

where s_o and t_o are s and t such that Eq. 7 is minimized. As is shown by Eq. 10, R_m is described as the ratio between N_m and the total number of pixels that are classified as belonging to the vein region in the two data sets.

4 Experimental results

This section describes the experiments we ran to evaluate the performance of the finger-vein-extraction algorithm. First we describe the determination of the number of times line tracking is repeated. Next we describe the accuracy of finger-vein extraction and the robustness of the algorithm against irregular shading in the captured images. Then we describe the experiment we performed using infrared finger images from 678 volunteers to investigate the applicability of this finger-vein-pattern-based method of identification. Finally, we evaluate the response time.

In the experiments, the finger images were captured using a grayscale, infrared-sensitive 1/2-in. CCD camera (NC300AIR, TAKEX). The resolution of the images was approximately 0.3 mm/pixel.

4.1 Determining number of times line tracking is repeated

To determine the appropriate number of line-tracking operations, we compared finger-vein patterns extracted using various numbers of line-tracking operations.

First, 16 finger-vein patterns were extracted from a captured image, each time using the proposed method with $N = 100$. Each pattern differed slightly from the others because the line-tracking operations are executed based on random numbers. Next, all finger-vein patterns were compared with each other in all combinations, and the differences were plotted on a graph. Finally, the procedure was repeatedly executed with an increased N ($100 \le N \le 10000$).

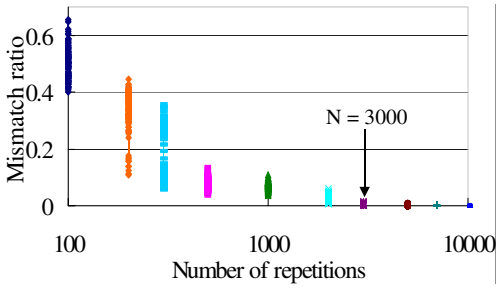

Fig. 6. Relationship between number of line-tracking operations and differences among finger-vein patterns extracted with same number of steps from same image

Figure 6 shows the relationship between the total number of line-tracking operations ($= N$) and the differences among finger-vein patterns extracted from the same image. The mismatch ratio is the difference between two patterns (Sect. 3.3.2).

When the number of line-tracking operations was relatively small (about $N \le 2000$), the mismatch ratio was large. This means that patterns are not extracted adequately when N is small. On the other hand, the mismatch ratio was small for larger N ($3000 \le N$). When N was 3000, the mismatch ratio was only about 0.5%. This means that the patterns were approximately the same for all images.

4.2 Accuracy of feature extraction

To determine whether the proposed method faithfully extracts the patterns of veins, we investigated the correlation between the patterns extracted with the proposed method and the actual patterns. We also compared the experimental results for a conventional method with those for the proposed method. The actual patterns were extracted by experts and then converted into binarized data.

The conventional method we used was matched filtering. The two-dimensional filter kernel is designed so that its profile matches the cross-sectional profile of a typical vein, like that shown in Fig. 3. An integer is selected for each value of a row element of the filter kernel such that the sum of the values in a given row is zero. All values in a given column of the filter kernel are the same, since this emphasizes the line-shaped features. A filter kernel based on the above principles is shown in Fig. 7.

The matched filters consist of four different filter kernels, with each filter rotated by 45° to optimize for a different set of vein directions. All the filters are independently convolved with the captured image, and the convolution values are added. Finally, the values are binarized using a threshold such that the dispersion between the two groups of convolution values is maximized.

In this experiment, we omitted spatial reduction and relabeling so that more accurate results were acquired using higher-resolution images. The size of the data was thus width

26	8	-18	-32	-18	8	26
26	8	-18	-32	-18	8	26
26	8	-18	-32	-18	8	26
26	8	-18	-32	-18	8	26
26	8	-18	-32	-18	8	26
26	8	-18	-32	-18	8	26
26	8	-18	-32	-18	8	26

Fig. 7. Matched filter designed by using the cross-sectional profile of a typical vein

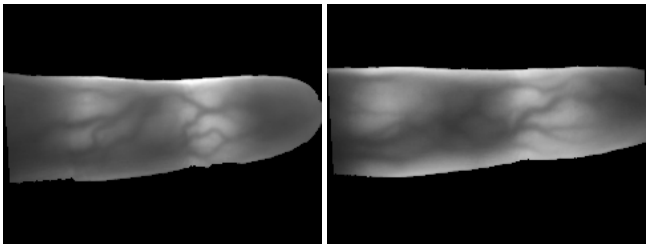

a **b**

Fig. 8a,b. Finger-vein images used in experiment. **a** Original image (1). **b** Original image (2)

$w = 240$ pixels, height $h = 180$ pixels, and moving distance $c_w = c_h = 10$, so that a displacement of the finger position by about 3 mm could be absorbed.

The experiment was carried out as follows using the two images shown in Figs. 8a and b.

Step 1: Acquisition of the infrared images
Step 2: Finger-vein extraction by hand
Step 3: Finger-vein extraction by conventional and proposed methods
Step 4: Creation of the data for use in matching from the patterns of finger veins extracted by each method
Step 5: Matching between the data created by hand and by the proposed method
Step 6: Matching between the data created by hand and by the conventional method

Figures 9 and 10 show the finger-vein patterns extracted from the images shown in Figs. 8a and b, respectively. Table 1 shows the results of matching.

We can see in Figs. 9 and 10 that the proposed method led to little excessive extraction, while there was excessive extraction and many thin spots along the veins in the images created using the conventional method. As shown in Table 1, the mismatch ratio between the patterns extracted using the conventional method and by hand was 44% on average, while that for the proposed method was 33%.

The conventional method emphasizes the depth of the intensity profile in the captured image. This leads to partial extraction of the desired features, but the line patterns may be blurred in the presence of irregular shading. Moreover, the noise is emphasized. On the other hand, the proposed method emphasizes the valleys in the cross-sectional profile through the repeated line-tracking operation. Therefore, it is robust against irregular shading, and the desired features are extracted evenly everywhere. Moreover, dots of noise are barely extracted because line connectivity is considered.

a **b** **c**

Fig. 9a–c. Finger-vein patterns extracted from Fig. 8a by hand-labeling, and using proposed and conventional methods. **a** Hand-labeled. **b** proposed method. **c** Matched filter

a **b** **c**

Fig. 10a–c. Finger-vein patterns extracted from Fig. 8b by hand labeling and using proposed and conventional methods. **a** Hand-labeled. **b** Proposed method. **c** Matched filter

Table 1. Results of matching vein patterns extracted using proposed and conventional methods with actual vein pattern

Image	Mismatch ratio	
	Proposed method	Conventional method
Image (1)	33.5%	47.0%
Image (2)	33.3%	40.3%

These results show that the proposed method is better in terms of robustness against irregular shading and noise and that it is capable of faithful feature extraction.

4.3 Robustness of feature extraction against irregular shading

Robust extraction of the finger-vein patterns in shadowy images is important. We examined the proposed method's robustness against the irregular shading by using images acquired at different infrared-LED light intensities and investigating the quality of the patterns extracted from them.

The matched-filter method was again used for comparison, and the spatial reduction and relabeling steps were again omitted.

This experiment was carried out as follows, with the proposed and conventional methods used independently.

Step 1: Capture infrared finger images using various LED light intensities within range where veins are visible.
Step 2: Use proposed method to extract finger-vein patterns from images.
Step 3: Compare each pattern with pattern obtained from brightest image and calculate mismatch ratio.
Step 4: Use conventional method to extract finger-vein patterns and calculate mismatch ratio in same way as in steps 2 and 3.

Figure 11a shows the brightest image, and Figs. 11b and c show the results of extraction from this image using the proposed and conventional methods, respectively. Figure 12

a **b** **c**

Fig. 11a–c. Results for extracted finger veins in the brightest infrared finger image. **a** Brightest image. **b** Proposed method. **c** Matched filter

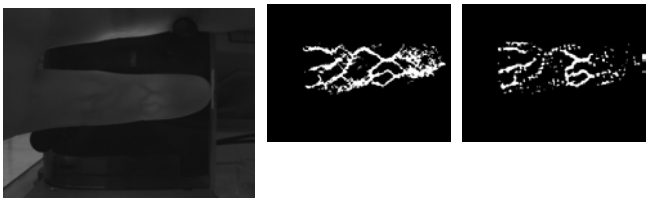

a **b** **c**

Fig. 12a–c. Results for extracted finger veins in the darkest infrared finger image. **a** Darkest image. **b** Proposed method. **c** Matched filter

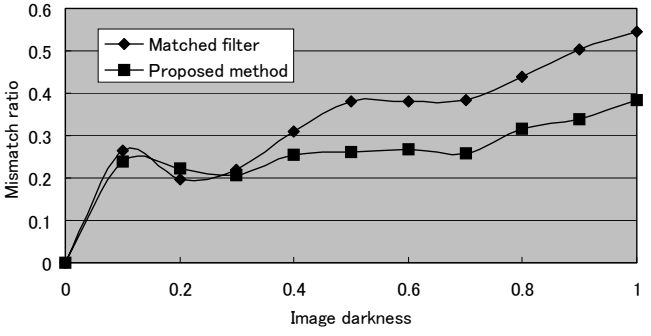

Fig. 13. Robustness against fluctuations in light-power level

shows the corresponding results for the darkest image. As shown in Fig. 12, the image extracted using the proposed method was clearer than that extracted using the conventional method.

Figure 13 shows the relationship between the mismatch ratio and the image darkness, defined as $1-(B_i-B_1)/(B_{11}-B_1)$, where B_i is the average intensity that is i-th darkest in the captured images ($i = 1, 2, ..., 11$); thus, $B_1 < B_2 < ... < B_{11}$. In this experiment, B_1 was 45 and B_{11} was 90. The mismatch ratio was obtained by calculating the difference between the finger-vein pattern extracted from each of the images and that extracted from the brightest image.

As the captured image became darker, the mismatch ratio increased for both methods. The maximum value for the proposed method was 39%, 13% less than the 52% obtained for the conventional method. Our method is thus more robust against LED light-intensity fluctuation.

4.4 Personal identification using finger-vein patterns

To examine our method's performance for personal identification, we did an experiment using the method to identify large numbers of patterns. The experiment involved evaluating the false acceptance (FAR) and false rejection (FRR) error rates for a database of infrared finger images. The database contained 678 different infrared images of fingers, with two images per finger. They were obtained from people working in our laboratory, ranging in age from 20s to 40s and approximately 70% men.

The FRR was obtained by calculating the mismatch ratios using both images of each finger, and the FRR was obtained by calculating the mismatch ratios among the images of different fingers for all combinations (678×677). The conventional method was independently evaluated in the same way.

The relationship between the mismatch ratios and the frequency is shown in Fig. 14. Each distribution was normalized by its maximum frequency. The averages of the distributions among different persons were high; the mismatch ratio was around 50% for both methods. Most values in the distributions for the same persons were low, although some were high because of a finger displacement.

The distributions for the same and different fingers were almost entirely separated from each other, showing that personal identification can be performed by using finger-vein patterns. The proposed method produced a smaller region of overlap between the two distributions, for the same and for different fingers, than did the conventional method.

To quantitatively evaluate these results, we calculated the equal error rate (EER), i.e., the rate of trials in which the FAR equaled the FRR. The method of calculating the EER is as follows. First, the threshold of the mismatch ratio (T_i) is defined as $T_i = i/1000 (i = 0, 1, ..., 1000)$. Next, the false rate ($\mathrm{FRR}_i$), which is defined as the ratio between the number of data on the same fingers for which the mismatch ratio is greater than T_i and the total number of data on the same fingers, is calculated for all i. Then, the false rate (FAR_i), which is defined as the ratio between the number of data on different fingers for which the mismatch ratio is less than T_i and the total number of data on different fingers, is calculated for all i. Finally, the EER is calculated by searching FAR_i so that $|\mathrm{FAR}_i - \mathrm{FRR}_i|$ is minimized, since a value i such that $\mathrm{FRR}_i = \mathrm{FAR}_i$ does not always exist because FRR_i and FAR_i are discrete numbers.

The receiver operating characteristic (ROC) curve, which shows the relationship between FAR and FRR, is shown in Fig. 15.

It shows that EER was 0.145% for a mismatch ratio of 37.6% when the proposed method was used, while it was 2.36% for a mismatch ratio of 38.4% when the conventional method was used. That is, the error rate in personal identification was smaller for the proposed method than for the conventional method. Therefore, the proposed method is more effective.

Furthermore, the EER for fingerprint-based systems has a range of 0.2 to 4% [9,10], meaning that finger-vein identification using the proposed method is highly effective.

4.5 Response time

To evaluate the response time, we measured the processing times for feature extraction and matching. The computer had a 550-MHz Pentium III CPU and 128 MB of memory. The application program was implemented in Visual C++ 6.0.

The average time for feature extraction was 450 ms, and that for matching was 10 s. That is, the total time for identifica-

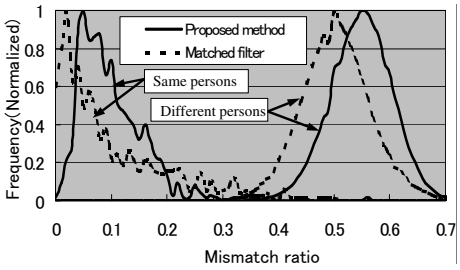

Fig. 14. Mismatch ratio for the same person and among different persons

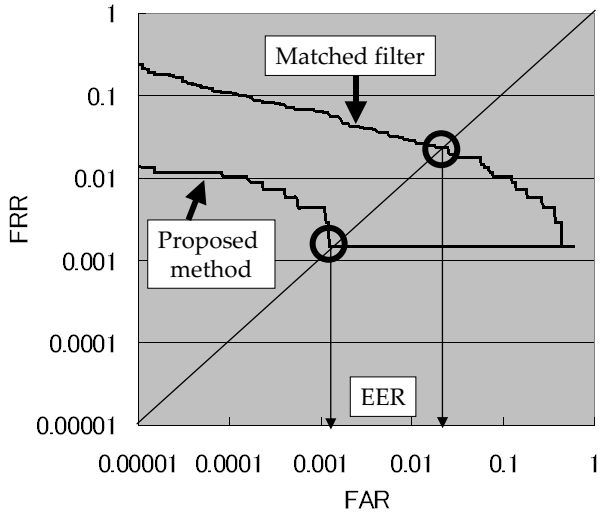

Fig. 15. ROC curve

tion was 460 ms per finger. The response time was thus within 0.5 s. In other words, the response time sufficiently satisfied the requirements for user convenience in terms of response time.

5 Conclusion

We described a personal identification method based on patterns of veins in a finger. To extract the patterns from an unclear original image, line-tracking operations with randomly varied start points are repeatedly carried out. Evaluation of its robustness against image darkness showed that it is far superior to the conventional method based on a matched filter. Further experiments showed that the equal error rate was 0.145% and the response time was 460 ms, which means the method is very effective as a means for personal identification.

Moreover, our method can be easily combined with other biometric techniques based on parts of the hand (fingerprints, finger/hand geometry, and so on). A multimodal identification system can thus be composed by using various methods while ensuring user convenience.

We plan to improve both the imaging device and algorithm to obtain an even higher recognition rate. More specifically, we will work on the following issues:

(1) Three-dimensional rotation of the finger degrades identification accuracy because two-dimensional images are used in this system. We plan to design a device that forces the user to place a finger in the same position every time.

(2) The mismatch ratio is slightly higher during cold weather because the veins of the finger can become unclear. Therefore, a device that can capture the vein pattern more clearly and a feature extraction algorithm that is robust against these fluctuations will be investigated.

Furthermore, we plan to develop an algorithm that can automatically evaluate the adequacy of the registered patterns.

Acknowledgements. We thank Dr. Shin-ichiro Umemura and Dr. Miyuki Kono for their many helpful suggestions and all the members of Hitachi CRL who allowed us to take infrared images of their fingers.

References

1. Shen W, Surette M, Khanna R (1997) Evaluation of automated biometrics-based identification and verification systems. In: Special issue on automated biometric systems. Proc IEEE 85(9):1463–1478
2. Kono M, Ueki H, Umemura S (2000) A new method for the identification of individuals by using vein pattern matching of a finger. In: Proceedings of the 5th symposium on pattern measurement, Yamaguchi, Japan, pp 9–12 (in Japanese)
3. Miura N, Nagasaka A, Miyatake T (2001) An extraction of finger vein patterns based on multipoint iterative line tracing. In: Proceedings of the 2001 IEICE general conference, Shiga, Japan, D-12-4 (in Japanese)
4. Hoover A, Kouznetsova V, Goldbaum M (2000) Locating blood vessels in retinal images by piece-wise threshold probing of a matched filter response. IEEE Trans Med Imag 19(3):203–210
5. Walter T, Klein J, Massin P, Zana F (2000) Automatic segmentation and registration of retinal fluorescein angiographies – application to diabetic retinopathy. In: Proceedings of the 1st international workshop on computer assisted fundus image analysis, Copenhagen, 29–30 May 2000, pp 15–20
6. Montesinos P, Alquier L (1996) Perceptual organization of thin networks with active contour functions applied to medical and aerial images. In: Proceedings of ICPR'96, Vienna, Austria, pp 25–30
7. Tsuda T (1995) Monte Carlo methods and simulation, 3rd edn. Baifukan, Tokyo
8. Nagao M (1983) Methods of image pattern recognition. Corona, San Antonio, TX
9. Jain AK, Pankanti S (2001) Automated fingerprint identification and imaging systems. In: Lee HC, Gaensslen RE (eds) Advances in fingerprint technology, 2nd edn. Elsevier, New York
10. Prabhakar S, Jain AK, Pankanti S (2003) Learning fingerprint minutiae and type. Pattern Recog 36(8):1847–1857
11. Maio D, Maltoni D (1997) Direct gray-scale minutiae detection in fingerprints. IEEE Trans Pattern Anal Mach Intell 19(1):27–40
12. Im S, Park H, Kim Y, Han S, Kim S, Kang C, Chung C (2001) A Biometric identification system by extracting hand vein patterns. J Korean Phys Soc 28(3):268–272
13. Jain AK, Ross A, Pankanti S (1999) A prototype hand geometry-based verification system. In: Proceedings of the 2nd international conference on audio- and video-based biometric person authentication. Washington DC, pp 166–171
14. Boles WW, Boashash B (1998) A human identification technique using images of the iris and wavelet transform. IEEE Trans Signal Process 46(4):1185–1188

15. Venayagamoorthy GK, Moonasar V, Sandrasegaran K (1998) Voice recognition using neural networks. In: Proceedings of the IEEE South African symposium on communication and signal processing (COMSIG 98), pp 29–32
16. Jain AK, Duin RPW, Mao J (2000) Statistical pattern recognition: a review. IEEE Trans Pattern Anal Mach Intell 22(1):4–37
17. Zhang W, Wang Y (2002) Core-based structure matching algorithm of fingerprint verification. In: Proceedings of the IEEE international conference on pattern recognition, 1:70–74
18. Chen X, Flynn PJ, Bower KW (2003) Visible-light and infrared face recognition. In: Proceedings of the workshop on multimodal user authentication, pp 48–55

Naoto Miura received B.E. and M.E. degrees from the University of Tokyo, Japan, in 1998 and 2000, respectively. Since 2000 he has been with the Central Research Laboratory of Hitachi Ltd. and is presently a researcher in the Ubiquitous Media Systems Research Department. His research interests include biometric identification, image processing, and pattern recognition.

Akio Nagasaka received B.E. and M.E. degrees from Hokkaido University, Japan, in 1989 and 1991, respectively. He joined the Central Research Laboratory of Hitachi Ltd. in 1991 and is presently a senior researcher in the Ubiquitous Media Systems Research Department. He has been active in the fields of real-time video-image processing, multimedia systems, and biometrics. He received a doctoral degree in electronics and information engineering from Hokkaido University in 2000. Since 2001, he has been a visiting associate professor at the Japan Advanced Institute of Science and Technology .

Takafumi Miyatake graduated from Tadotsu Technical High School, Kagawa, Japan, in 1971 and from Hitachi Technical College, Kanagawa, Japan, in 1973. Since 1971 he has been with the Central Research Laboratory of Hitachi Ltd. and is presently a senior researcher in the Ubiquitous Media Systems Research Department. He has participated in R&D activities in the fields of 3D object recognition, drawing recognition, and real-time video analysis; his current interest is extended image processing for security systems. From 1981 to 1982 he was a visiting researcher at Kyoto University, Kyoto, Japan. He received a doctoral degree in information engineering from the University of Tokyo in 1996. He is a member of the Institute of Image Information and Television Engineers, Tokyo, Japan.